

Decoherence in a Cooper pair shuttle

Alessandro Romito, Francesco Plastina, and Rosario Fazio
NEST-INFM & Scuola Normale Superiore, I-56126 Pisa, Italy
(Dated: November 29, 2018)

We examine decoherence effects in the Josephson current of a Cooper pair shuttle. Dephasing due to gate voltage fluctuations can either suppress or enhance the critical current and also change its sign. The current noise spectrum displays a peak at the Josephson coupling energy and shows a phase dependence.

PACS numbers:

The Josephson effect¹ consists in a dissipation-less current between two superconducting electrodes connected through a weak link^{2,3}. The origin of the effect stems from the macroscopic coherence of the superconducting condensate. Since its discovery in 1962, the research on devices based on the Josephson effect has been achieving a number of important breakthroughs both in pure² and applied physics³. One of the most recent exciting developments is probably the implementation of superconducting nano-circuits for quantum information processing⁴, which requires the ability to coherently manipulate these devices. By now, this has been shown in several experiments in systems of small Josephson junctions⁵.

Very recently, Gorelik *et al.*^{6,7} proposed a very appealing setup, the Cooper pair shuttle, able to create and maintain phase coherence between two distant superconductors. In its simplest realization, shown in Fig.1, the system is made up of a superconducting grain, externally forced to move periodically between two superconducting electrodes. Despite the fact that the grain is in contact with only one lead at a time, the shuttle does not only carry charge, as in the normal metal case^{8,9,10}, but it also establishes phase coherence between the superconductors.

Aim of this work is to analyze how the presence of the environment affects the coherent transport in the Cooper pair shuttle. The interplay¹¹ between the periodic driving and the environmental dephasing leads to several interesting results. By increasing the coupling to the environment it may result in an *enhancement* of the supercurrent as well as in a change of its sign (π -junction). In the last part of this Letter we propose an effective implementation of the shuttle mechanism where the switching of the Josephson couplings is controlled by an external magnetic field. The shuttle consists of a small superconducting island coupled to two macroscopic leads and forced to change its position periodically in time, with period T , from the Right (R) to the Left (L) electrode and back (see Fig.1). The grain is small enough so that charging effects are important, while the two leads are macroscopic and have definite phases $\phi_{L,R}$. The moving island is described by the Hamiltonian

$$H_0 = E_C [\hat{n} - n_g(t)]^2 - \sum_{b=L,R} E_J^{(b)}(t) \cos(\hat{\phi} - \phi_b) \quad (1)$$

where E_C is the charging energy, $E_J^{(L,R)}$ is the Josephson coupling to the left or right lead respectively, and n_g is the gate charge. The variable \hat{n} is the number of excess Cooper pairs in the grain and $\hat{\phi}$ is its conjugate phase, $[\hat{n}, \hat{\phi}] = -i$. The system operates in the Coulomb blockade regime, $E_J^{(b)} \ll E_C$ ($b = R, L$) so that only the two charge states $\{|n=0\rangle, |n=1\rangle\}$ are important. Their relative energy (ΔE_C) is controlled by the gate charge $n_g(t)$. The superconducting gap is assumed to be the largest energy scale in the problem, so that quasiparticle tunnelling can be neglected. Both E_C and $E_J^{(L,R)}$ are time dependent: when the grain is close to one of the leads, the corresponding Josephson coupling is non-zero (with value E_J) and the two charge states are degenerate (positions L and R in Fig.1). In the intermediate region (position C), $E_J^{(L)} = E_J^{(R)} = 0$. As in Ref.⁷ we employ a sudden approximation (which requires a switching time $\Delta t \ll 1/E_J$) and suppose $E_J^{(L,R)}(t)$ to be step functions

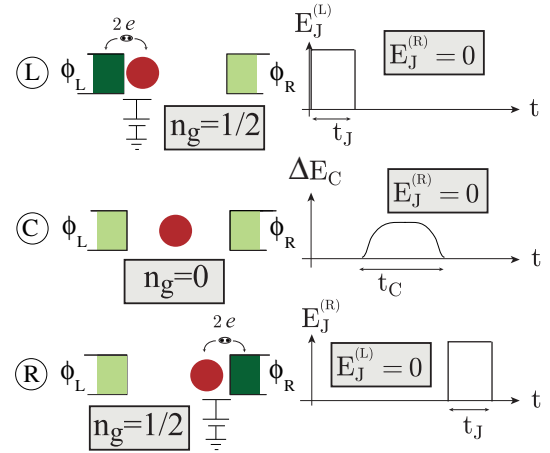


Figure 1: Time dependence of the Josephson and charging energies in the Cooper pair shuttle. The three intervals L, C and R, within the period $T = 2t_J + 2t_C$, correspond to the situations: **L**) represents $E_{JL} = E_J$, $n_g = 1/2$, $E_J^{(R)} = 0$ (interaction time); **C**) represents $E_J^{(L)} = 0$, $n_g = 0$, $E_J^{(R)} = 0$ (free evolution time); **R**) $E_J^{(L)} = 0$, $n_g = 1/2$, $E_{JR} = E_J$ (interaction time). On the left hand side, the corresponding position of the shuttle with respect to the leads is shown for each time interval.

in each region (see Fig.1). We further assume, as in Ref.⁶, that the system is at the charge degeneracy as long as the island is in contact with one of the electrodes. In the intermediate region (C) it is not necessary to specify the exact variation of $n_g(t)$, only the time integral of the energy difference between the two charge states will enter in the results.

The shuttle is coupled via the charge operator \hat{n} to an environment described by the Caldeira–Leggett model¹²

$$H_{int} = \hat{n} \sum_i \lambda_i (a_i + a_i^\dagger) + H_{bath}. \quad (2)$$

In Eq.(2), H_{bath} is the bath Hamiltonian, with boson operators a_i, a_i^\dagger for its i -th mode. The form of the coupling in Eq.(2) can describe either gate voltage fluctuations⁴ or, in some limits, random switching of background charges in the substrate¹³.

In order to analyze the transport process, we evaluate the time averaged supercurrent at steady state

$$I = \overline{\langle \hat{I} \rangle} \equiv \frac{1}{T} \int_0^T dt \langle \hat{I}(t) \rangle, \quad (3)$$

and the power spectrum of the current fluctuations

$$S(\omega) = \int_{-\infty}^{+\infty} d\tau \tilde{S}(\tau) e^{-i\omega\tau} \quad (4)$$

where

$$\tilde{S}(\tau) = \frac{1}{2} \overline{\langle [\hat{I}(t+\tau), \hat{I}(t)] \rangle_+} - \overline{\langle \hat{I}(t+\tau) \rangle \langle \hat{I}(t) \rangle}. \quad (5)$$

In the Schrödinger picture, the current operator is ($\hbar = 1$)

$$\hat{I}(t) = 2eE_J \sin(\hat{\varphi} - \phi_L) \Theta_L(t) \quad (6)$$

corresponding to the exchange of Cooper pairs with the left lead. The function $\Theta_L(t)$ is defined as follows: $\Theta_L(t) = 1$ when the grain is in the L region, and $\Theta_L(t) = 0$ otherwise (the functions $\Theta_R(t)$ and $\Theta_C(t)$ are defined analogously). In order to evaluate Eqs.(3, 4), we need to compute the reduced density matrix of the grain $\rho(t)$. After one period the evolution of $\rho(t)$ can be computed through a map \mathcal{M}_t defined by $\rho(t+T) = \mathcal{M}_t \rho(t)$. The stationary limit is obtained by studying the fixed point of \mathcal{M}_t ¹⁴. Since only two charge states in the grain are relevant, the reduced density matrix can be parametrized, in the charge basis, as $\rho(t) = 1/2 [\mathbb{I} + \vec{\sigma} \cdot \vec{r}(t)]$, where σ_i ($i = x, y, z$) are the Pauli matrices and $r_i(t) = \langle \sigma_i \rangle$. The assumption of a stepwise varying Hamiltonian considerably simplifies the form of the map \mathcal{M}_t , obtained as a composition of the time evolutions of ρ in the intervals L,C,R (see Fig. 1). Separately for each of these intervals, the master equation for $\vec{r}(t)$ has the form¹⁵

$$\dot{\vec{r}}(t) = \sum_{k \in \{L, R, C\}} [G_k(t) \vec{r}(t) + 2\gamma_J(T_b) \vec{w}_k] \Theta_k(t) \quad (7)$$

with $\vec{w}_{L,R}^\dagger = \tanh(E_J/T_b) (\cos \phi_{L,R}, \sin \phi_{L,R}, 0)$, $\vec{w}_C^\dagger = (0, 0, 0)$,

$$G_{L,R} = \begin{pmatrix} -2\gamma_J(T_b) & 0 & -E_J \sin \phi_{L,R} \\ 0 & -2\gamma_J(T_b) & -E_J \cos \phi_{L,R} \\ E_J \sin \phi_{L,R} & E_J \cos \phi_{L,R} & 0 \end{pmatrix}, \quad (8)$$

$$G_C = \begin{pmatrix} -\gamma_C(T_b) & -E_C & 0 \\ E_C & -\gamma_C(T_b) & 0 \\ 0 & 0 & 1 \end{pmatrix}, \quad (9)$$

where the bath is taken in thermal equilibrium at temperature T_b .

Here, $\gamma_J(T_b)$ and $\gamma_C(T_b)$ are the temperature-dependent dephasing rates in the regions L, R and C, respectively, obtained in the Born-Markov approximation. As an example, for an ohmic bath with coupling to the environment $\alpha \ll 1$, one has¹² $\gamma_J(T_b) = (\pi/2)\alpha E_J \coth(E_J/2T_b)$ and $\gamma_C(T_b) = 2\pi\alpha T_b$. This treatment is valid provided that $\gamma_{J,C} \ll T_b, E_J$, and that the time interval $t_{J(C)}$ is much longer than both T_b^{-1} and $E_{J(C)}^{-1}$. In the coupling regions L and R, the only energy scale is set by the Josephson energy, while, during the free evolution time, the relevant scale is the energy difference between charge states. Correspondingly, all the physical quantities depend on the phases $2\theta = E_J t_J$ and $2\chi = \int_C dt \Delta E_C(t)$ ¹⁶. The other important variable is the phase difference $\phi = \phi_L - \phi_R$. The effect of damping is characterized by the two dimensionless quantities $\gamma_J t_J$ and $\gamma_C t_C$ ¹⁷.

Average current- In the limiting case considered by Gorelik *et al.*⁶, the Josephson current does not depend on the dephasing rates. One expects, however, that this cannot be always the case. If, for example, the period T is much larger than the inverse dephasing rates, the shuttle mechanism is expected to be inefficient and the critical current should be strongly suppressed. In fact, we find a quite rich scenario, depending on the relative value of the various time scales and phase shifts.

The expression of the current $I(\phi, \theta, \chi, \gamma_J t_J, \gamma_C t_C)$ can be obtained analytically from Eqs.(3,7). However, it is rather cumbersome and not instructive, so we prefer to present it in some limiting cases. A typical plot of I as a function of θ and ϕ is shown in Fig.2. Depending on the value of θ (a similar behaviour is observed as a function of χ), the critical current can be negative, i.e. the system can behave as a π -junction. The phase shifts accumulated in the time intervals L,C and R, leading to the current-phase relation shown in Fig.2, are affected by the dephasing rates in a complicated way. By changing $\gamma_J t_J$ and $\gamma_C t_C$, certain interference paths are suppressed, resulting in a shift of the interference pattern and ultimately in a change of the sign of the current, as shown in Fig.3.

An analysis of the critical current as a function of the dephasing rates reveals another interesting aspect: the Josephson current is a non-monotonous function of $\gamma_J t_J$, i.e. by *increasing* the damping, the Josephson current

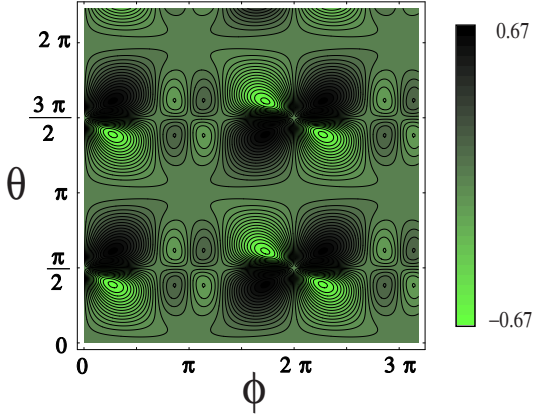


Figure 2: Supercurrent (in units of e/T) as a function of the superconductor phase difference ϕ and of the phase accumulated during the contact to one of the electrodes θ . The other parameters are fixed as: $\chi = 5\pi/6$, $e^{-\gamma_J t_J} = 3/4$, $e^{-\gamma_C t_C} = 4/5$. The plot is obtained for $T_b \ll E_J$

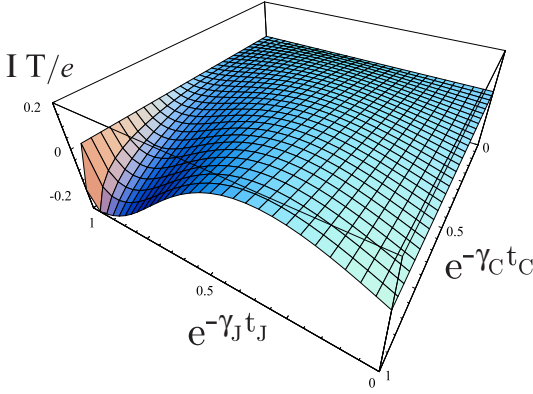


Figure 3: Average current ($T_b \ll E_J$) as a function of the dephasing rates, with $\phi = -3\pi/4$, $\theta = 7\pi/10$, $\chi = 5\pi/6$. As a function of $\gamma_J t_J$, the supercurrent has a non-monotonic behavior. Note the change of sign in the current obtained by varying decoherence rates in each time interval separately.

can *increase*. The behavior as a function of the dephasing rates is presented in Fig.3. The presence of a maximum Josephson current at a finite value of $\gamma_J t_J$ can be understood by analyzing the asymptotic behaviors in the strong and weak damping limits, where simple analytic expressions are available (in the following we do not explicitly write the temperature dependence in γ_J , γ_C).

i) If the dephasing is strong, I can be expanded in powers of $e^{-\gamma_J t_J}$ and $e^{-\gamma_C t_C}$ and, to leading order

$$I_{strong} \sim \frac{2e}{T} \tanh\left(\frac{E_J}{T_b}\right) e^{-(\gamma_J t_J + \gamma_C t_C)} \cos(2\chi) \sin(2\theta) \sin\phi. \quad (10)$$

Strong dephasing is reflected in the simple (i.e. $\propto \sin\phi$) current-phase relationship and in the exponential suppression of the current itself.

ii) In the opposite limit of weak damping ($\gamma_J t_J \ll$

$\gamma_C t_C \ll 1^{17}$),

$$I_{weak} \sim \frac{2e}{T} \tanh\left(\frac{E_J}{T_b}\right) \frac{\gamma_J t_J}{\gamma_C t_C} \frac{(\cos\phi + \cos 2\chi) \tan\theta \sin\phi}{1 + \cos\phi \cos 2\chi}. \quad (11)$$

The current tends to zero if the coupling with the bath is negligible during the interaction time. In this case, indeed, the time evolution in the intervals L, R is almost unitary, while, in the region C , pure dephasing leads to a suppression of the off-diagonal terms of the reduced density matrix $\rho(t)$. As a result, in the stationary limit the system is described by a complete mixture with equal weights. The current then tends to zero in both limiting cases of large and small $\gamma_J t_J$. Therefore one should expect an optimal coupling to the environment where the Josephson current is maximum. A regime where the crossover between the strong and weak damping cases can be described in simple terms is the limit $\gamma_C \rightarrow 0$, for a fixed value of θ . For example, at $\theta = \pi/4$ the current reads

$$I = \frac{2e}{T} \tanh\left(\frac{E_J}{T_b}\right) \times \frac{2e^{-\gamma_J t_J} [2e^{-2\gamma_J t_J} \cos\phi + (1 + e^{-4\gamma_J t_J}) \cos 2\chi] \sin\phi}{(1 + e^{-2\gamma_J t_J})(1 + e^{-2\gamma_J t_J} \cos\phi \cos 2\chi + e^{-4\gamma_J t_J})} \quad (12)$$

In the limit of vanishing $\gamma_J t_J$, Eq.(12) corresponds to the situation discussed in⁶. Indeed, both expressions are independent of the dephasing rates. The difference in the details of the current-phase(s) relationship are due to the different environment.

In all the three cases presented here, Eqs.(10,11,12), the change of sign of the current as a function of the phase shifts θ or χ is evident.

Current Noise - Cooper pair shuttling is a result of a non equilibrium steady state process. Therefore, to better characterize the transport, we analyze supercurrent fluctuations as defined in Eq.(4). This should be contrasted with the standard Josephson effect², where the supercurrent is an equilibrium property of the system. We first consider the zero frequency noise in the two regimes of strong and weak dephasing.

When the dephasing is strong, correlations on time scales larger than T are suppressed and the noise spectrum reads

$$S(0)_{strong} \sim \frac{4e^2}{T} \left\{ \frac{1}{2} - e^{-\gamma_J t_J} \cos(2\theta) + e^{-2\gamma_J t_J} f(\theta, \phi, \chi) \right\}, \quad (13)$$

where $f(\theta, \phi, \chi) = \cos^2(2\theta) - e^{-\gamma_C t_C} \cos\phi \cos\chi \sin^2(2\theta)$. The leading term in Eq.(13) is due to the damped oscillations in the contact regions (L,R). The phase dependent contribution is exponentially suppressed since it comes from correlations over times larger than the period. For weak dephasing (same limits of Eq. (11)), we find

$$S(0)_{weak} \sim \frac{4e^2}{T} \frac{1}{\gamma_C t_C} \frac{\tan^2\theta \sin^2\phi}{2(1 + \cos\phi \cos 2\chi)}, \quad (14)$$

which shows a much richer structure as a function of the phases θ and χ ¹⁸. Finally, we briefly discuss the finite frequency spectrum in the case of strong dephasing (see Fig.4). Superimposed to the peak at the Josephson

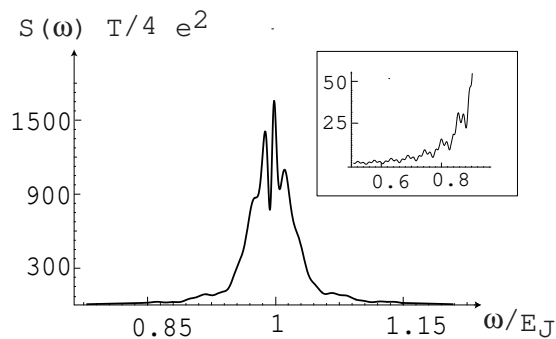


Figure 4: Current noise spectrum as a function of ω for $T = 4t_J$ in strong dephasing limit ($\gamma_J t_J = 1.2$ and $\gamma_J/E_J = 0.008$). In the inset, we plot the spectrum in a restricted range of frequencies to better resolve the oscillations.

energy, there are oscillations of frequency of the order of T^{-1} . The presence of these oscillations is related to the periodicity of the island motion. The modification of these fringes as a function of the phases is a signature of the coherence in the Cooper pair shuttle.

We conclude by suggesting a possible experimental test of our results which does not require any mechanically moving part. The time dependence of the Josephson couplings and n_g is regulated by a time dependent magnetic field and gate voltage, respectively. The setup consists of a superconducting nanocircuit in a uniform magnetic field as sketched in Fig.5. By substituting the Josephson junction by SQUID loops, it is possible to control the E_J by tuning the applied magnetic field piercing the loop. The presence of three type of loops with different area, A_L, A_R, A_C allows to achieve independently the three cases, where one of the two E_J 's is zero (regions L,R) or both of them are zero (region C), by means of a *uniform* magnetic field. If the applied field is such that a half-flux quantum pierces the areas A_L, A_R or A_C , the Josephson couplings will be those of regions R,L and C, respectively and the Hamiltonian of the system can be exactly mapped onto that of Eq.(1). Moreover, by choosing the ratios $A_C/A_R = 0.146$, and $A_C/A_L = 0.292$ the two

Josephson coupling are equal, $E_J^{(L)} = E_J^{(R)}$. This implementation has several advantages. It allows to control the coupling with the environment by simply varying the time dependence of the applied magnetic field. The time scale for the variation of the magnetic field should be controlled at the same level as it is done in the implementation of Josephson nanocircuits for quantum computation (see Ref.⁴ for an extensive discussion). For a quantitative comparison with the results described here, the magnetic field should vary on a time scale shorter than \hbar/E_J , typically a few nanoseconds with the parameters of the first article in Ref.⁵. This is possible with present day technology¹⁹. At a qualitative level the results presented in this paper (π -junction behavior, non-monotonous behavior in the damping) do not rely on the step-change approximation of the Josephson couplings (which leads to Eq.(7)).

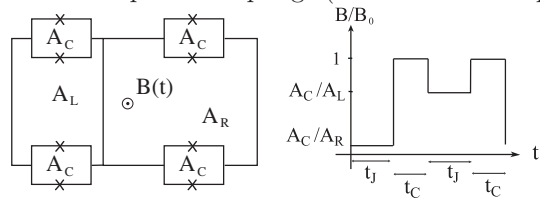


Figure 5: *left*: Sketch of the implementation of the shuttle process by means of a time-dependent magnetic field. Crosses represent Josephson junctions. *right*: Plot of the time variation of the applied field (in unity of $B_0 = \Phi_0/(2A_C)$, Φ_0 is the flux quantum) in order to realize the Cooper pair shuttle. The different loop areas can be chosen in order to obtain $E_J^{(L)} = E_J^{(R)}$.

Those effects are observable even if the magnetic field changes on time-scales comparable or slower than E_J . The only strict requirement is that only one Josephson coupling at the time is switched on.

We gratefully acknowledge many helpful discussions with G. Falci, Yu. Galperin and Yu.V. Nazarov. This work was supported by the EU (IST-SQUBIT, HPRN-CT-2002-00144) and by Fondazione Silvio Tronchetti Provera.

¹ B.D. Josephson, Phys. Lett. **1**, 251 (1962).

² M. Tinkham, *Introduction to Superconductivity*, (McGraw-Hill, New York, 1996).

³ A. Barone and G. Paternò, *Physics and Applications of the Josephson Effect*, (J. Wiley, New York, 1982).

⁴ Y. Makhlin, G. Schön and A. Shnirman, Rev. Mod. Phys. **73**, 357 (2001) and references therein.

⁵ Y. Nakamura, Yu.A. Pashkin, and J.S. Tsai, Nature **398**, 786 (1999); J.R. Friedman, V. Patel, W. Chen, S.K. Tolpygo, and J.E. Lukens, ibid. **406**, 43 (2000); C.H. van der Wal, A.C.J. ter Haar, F.K. Wilhelm, R.N. Schouten, C. Harmans, T.P. Orlando, S. Lloyd, and J.E. Mooij, Science **290**, 773 (2000); D. Vion, A. Aassime, A. Cottet, P. Joyez,

H. Pothier, C. Urbina, D. Esteve, and M.H. Devoret, ibid. **296**, 886 (2002); Y. Yu, S.Y. Han, X. Chu, S.I. Chu, and Z. Wang, ibid. **296**, 889 (2002); J.M. Martinis, S. Nam, J. Aumentado, and C. Urbina, Phys. Rev. Lett. **89**, 117901 (2002).

⁶ L. Y. Gorelik, A. Isacsson, Y. M. Galperin, R. I. Shekhter, and M. Jonson, Nature **411**, 454 (2001).

⁷ A. Isacsson, L. Y. Gorelik, R. I. Shekhter, Y. M. Galperin, and M. Jonson, Phys. Rev. Lett. **89**, 277002 (2002).

⁸ L. Y. Gorelik, A. Isacsson, M. V. Voinova, B. Kasemo, R. I. Shekhter, and M. Jonson, Phys. Rev. Lett. **80**, 4526 (1998).

⁹ A. Erbe, C. Weiss, W. Zwerger, and R.H. Blick, Phys. Rev.

- Lett. **87**, 096106 (2001).
- ¹⁰ D.L. Klein, R. Roth, A.K.L. Lim, A.P. Alivisatos, and P.L. McEuen, *Nature* **389**, 699 (1997).
- ¹¹ M. Grifoni and P. Hänggi, *Phys. Rep.* **304**, 299 (1998).
- ¹² U. Weiss *Quantum Dissipative Systems*, (World Scientific, Singapore, 1999).
- ¹³ E. Paladino, L. Faoro, G. Falci, and R. Fazio, *Phys. Rev. Lett.* **88**, 228304 (2002).
- ¹⁴ A. V. Shytov, D. A. Ivanov, M. V. Feigel'man, *cond-mat/0110490*.
- ¹⁵ C. Cohen-Tannoudji, J. Dupont-Roc, and G. Grynberg, *Atom-Photon Interactions*, Wiley, New York (1992).
- ¹⁶ A difference in the angles θ_L and θ_R leads only to quantitative changes with respect to the idealized case discussed in the paper; A Romito *at al.* (unpublished).
- ¹⁷ For some parameter values (e.g. $(\gamma_J, \gamma_C) = (0, 0)$ or $(\gamma_J, \theta) = (0, \pi/2)$) our model of the environment is not effective; i.e. the system keeps memory of its initial conditions and the expressions given in the text cannot be used. Experimentally, other sources of dissipation are present which will matter for these parameter values.
- ¹⁸ The general expression for the spectrum exhibits a divergence also in the limit $(\gamma_J, \theta) \rightarrow (0, k\pi/2)$ due to the increasingly longer correlation time of the current fluctuations (see ¹⁷).
- ¹⁹ O. Buisson, F. Balestro, J. Pekola, F.W.J. Hekking, *Phys. Rev. Lett.* **90** 238304 (2003); F. Balestro, PhD thesis Université Joseph Fourier, Grenoble (unpublished).